Orbiting resonance model for recombination of physisorbed atoms

Carey Schwartz and Robert J. Le Roy
Guelph-Waterloo Centre for Graduate Work in Chemistry, University of Waterloo, Waterloo, Ontario N2L 3G1, Canada

(Received 24 February 1984; accepted 7 June 1984)

The orbiting resonance model for atomic recombination, originally developed for applications to gas phase kinetics, is adapted for describing the recombination of atoms physisorbed on a surface. The model assumes that a population of atoms is initially physisorbed on a surface on which the atoms are free to move about in two dimensions. Atom–atom collisions give rise to long-lived orbiting pairs, which may in turn lose internal energy and become truly bound. The surface lowers the dimensionality of the problem, plays the role of the third body whose participation preserves energy and momentum conservation, and its corrugation provides the perturbation driving the second (inelastic) step of the mechanism. The present work involves the application of this model to the recombination of H or D atoms on the (111) and (100) surfaces of a Xe crystal, to obtain overall second-order rate constants at $T = 4$ and 10 K.

I. INTRODUCTION

It is well known that the rates of chemical reactions are often greatly affected by the presence or absence of a surface.[1–10] However, there is as yet little quantitative understanding of this phenomenon. In this communication we begin to address this problem by taking a model for a simple type of gas phase reaction, atomic recombination, and adapting it to describe the analogous reaction occurring on a surface, while taking as full account as possible of the effects due to the nature of the surface. The example for which detailed predictions are made is the recombination of H or D atoms which are physisorbed on the surface of a xenon crystal. This choice was made both because hydrogen recombination is a prototype reaction which has been extensively studied in the gas phase,[11–14] and because all of the relevant atom–atom pair potentials are well known. Other considerations include the lively current interest in two dimensional spin-polarized atomic hydrogen,[15,16] which is subject to the mechanism we propose, and the fact that the mechanism we discuss could be applicable to the formation of interstellar H_2.[17]

The mechanism explored here is the analog of the orbiting resonance model developed by Roberts, Curtiss, and Bernstein[18] for three-body gas phase recombination. Note, however, that the validity of the present work does not depend on whether or not this mechanism is dominant either in the gas phase[19] or on the surface. The basic premise of the model is that two atoms initially form a metastable state as a result of a two-body collision, after which a collision with a "third body" causes the metastable state to relax to a stable truly bound state. In the present case, the corrugation of the surface plays the role of the third body by providing the perturbation which drives the relaxation step. In addition, it alters the interaction energy between the adatom pair.

The present study focuses on the recombination step itself and does not consider either alternative mechanisms or subsequent or related processes, such as the coupling of the adatoms to the bulk and/or surface phonons of the substrate. The atoms under consideration are assumed to be already physisorbed on and in thermal equilibrium with the surface. By ignoring any coupling to the phonons, the atoms and any metastable adatom pairs will not desorb from the surface. In addition, as a matter of convenience we restrict our numerical results to "low" temperatures and low adatom concentrations both because this is where the present mechanism is more likely to be relatively important, and so that essential features of the physics, such as the dependence of the recombination rate upon the crystal structure, may be more readily discerned.

II. OVERVIEW OF THE MECHANISM

A. In the gas phase

This section briefly reviews the orbiting resonance model for gas phase atomic recombination, and describes how it is altered when the reaction is constrained to occur on a surface. The goal of the model was to predict the rate constant of the overall reaction

$$X + X + M \xrightarrow{k} X_2 + M\,, \tag{1}$$

where X_2 is the species undergoing recombination and M is a third body whose participation is required by the need to conserve energy and momentum. In the orbiting resonance model, the reaction of Eq. (1) is assumed to proceed via the mechanism:

$$X + X \underset{k_b^m}{\overset{k_f^m}{\rightleftharpoons}} X_2^*(m)\,, \tag{2}$$

$$X_2^*(m) + M \xrightarrow{k_r^{m,s}} X_2(s) + M\,, \tag{3}$$

where $X_2^*(m)$ is the metastable diatom in state m with energy $E > 0$ and $X_2(s)$ is the stable species (with energy $E < 0$) formed by the relaxation step. As implied above, the zero of energy is assumed to lie at the dissociation limit. Assuming that a steady state concentration of the metastable species is achieved, the overall rate constant is given by

$$k = \sum_{m,s} \frac{k_f^m k_r^{m,s}}{k_b^m + k_r^{m,s}[M]} = \sum_{m,s} \frac{K_e^m k_r^{m,s}}{(1 + k_r^{m,s}[M]/k_b^m)}\,, \tag{4}$$

 0021-9606/84/214149-11$02.10

where the sum is over all stable (s) and metastable (m) states of the product molecule X_2. In the limit when reaction (3) is much slower than the reverse of reaction (2), i.e., $k_b^m \gg k_r^{m,s}[M]$, this expression becomes

$$k = \sum_{m,s} K_e^m k_r^{m,s}, \tag{5}$$

where $K_e^m = k_f^m / k_b^m$ is the equilibrium constant associated with reaction (2). This equilibrium constant is defined by the properties of the metastable species m, from which its values may be readily calculated using elementary statistical mechanics.[20] Thus, once the relevant metastable states are identified and characterized, the required equilibrium constant values are easily obtained.

In the orbiting resonance theory, these metastable states are assumed to be the quasibound or orbiting resonance levels of the diatom pair. These levels lie above the asymptote of the potential energy function, but are classically bound by a potential energy barrier located at relatively large separations. Quantum mechanics allows such species to dissociate by tunneling through this potential energy barrier, and the rate constant k_b^m of Eq. (2) is therefore just the inverse of the associated tunneling lifetime. Formation of these metastable states is then possible only if atomic collisions occur at appropriate impact parameters and within narrow energy intervals about these resonance energies, where the widths of these intervals (the level widths) are of course related to the tunneling lifetime by the Heissenberg uncertainty principle. In any case, standard numerical methods allow one to routinely calculate the energies and tunneling lifetimes of all such levels for virtually any given effective one-dimensional potential.[21–23]

Calculating a rate constant from Eq. (5) requires estimates of both the equilibrium constant K_e^m and the rate constant $k_r^{m,s}$ of Eq. (3). In the gas phase case, the latter may be obtained from an exact or approximate scattering theory calculation, which in turn requires some estimate of the interaction potential between the metastable pair and the third body M. The sums of Eq. (5) are then easily performed, as a combination of level width and Boltzmann factor considerations imply that only a small number of metastable levels may contribute to this process.

B. On the surface

In the present case we assume that the recombining atoms are initially physisorbed on the surface. Since the corrugation of the surface plays the role of the third body M, it is always present. The overall reaction

$$X + X \xrightarrow{k} X_2 \tag{6}$$

proceeds sequentially as before, except that the first step [Eq. (2)] now involves atoms moving in two dimensions, and the relaxation step is now the first-order process

$$X_2^*(m) \xrightarrow[\text{surface}]{k_r^{m,s}} X_2(s) \tag{7}$$

driven by the corrugation of the surface. The overall mechanism is thus identical to the one given above, except that the final step does not explicitly involve a third body M. Assuming once again a steady state concentration of the metastable species $X_2^*(m)$, the rate constant for the overall reaction is given by

$$k = \sum_{m,s} K_e^m k_r^{m,s} \Big/ (1 + k_r^{m,s}/k_b^m). \tag{8}$$

Here, however, K_e^m represents the equilibrium between the physisorbed atoms and the physisorbed metastable molecules, and its values differ from those for the three dimensional gas phase system. Moreover, the rate constant $k_r^{m,s}$ may be obtained from a simple golden rule treatment, since the relaxation process is assumed to be a simple first-order process driven by the corrugation of the surface.

We demonstrate below that the substrate plays an important role in the recombination mechanism. First of all, the binding to the surface removes one degree of freedom from the motion of each adsorbed atom and two degrees of freedom from that of the molecule, in that each atom is assumed to be restricted to a plane parallel to the surface. Both the wave functions and the partition functions for the physisorbed species are therefore different than in the gas phase. These differences manifest themselves both in the values of the equilibrium constants and in the properties of the metastable and stable diatom states. The presence of the surface also allows for conservation of momentum and energy, and supplies the perturbation which drives the transition from metastable to stable levels of the molecule. This perturbation will be seen to arise from the nature of the atom–surface potential. A more subtle effect is that the presence of a material (the surface) with finite response to an electric field alters the atom–atom interaction. This is a consequence of maintaining the surface as an equipotential,[24] and implies that there are now additional contributions to the induced dipole–induced dipole interaction between the atoms. We see, however, that while the surface plays a vital role, the structure of the rate constant expressions remains the same as in the gas phase case.

III. DETAILS OF THE MODEL

A. Quantum mechanics of the physisorbed species

It is assumed that the substrate consists of a periodic array of identical particles which occupy the half-space corresponding to $z < 0$. The jth physisorbed atom ($j = 1,2$) has mass m_j and is located at position $\mathbf{r}_j = (\mathbf{R}_j, z_j)$, where $\mathbf{R}_j$ is a vector in the plane of the surface and z_j is the coordinate normal to the surface (see Fig. 1). The Hamiltonian for two such atoms is then

$$H = -\frac{\hbar^2}{2m_1}\nabla_1^2 - \frac{\hbar^2}{2m_2}\nabla_2^2 + V_{as}(\mathbf{r}_1) + V_{as}(\mathbf{r}_2) + V_{aa}(|\mathbf{r}_1 - \mathbf{r}_2|) + \Delta V_{aa}(\mathbf{r}_1, \mathbf{r}_2). \tag{9}$$

The first two terms in Eq. (9) represent the kinetic energies of the atoms, which are assumed to be able to move freely in two dimensions, while the next two represent the interaction energies between these atoms and the surface. The last two terms then represent, respectively, the free space atom–atom interaction and the modification of this pair potential due to surface mediated effects.

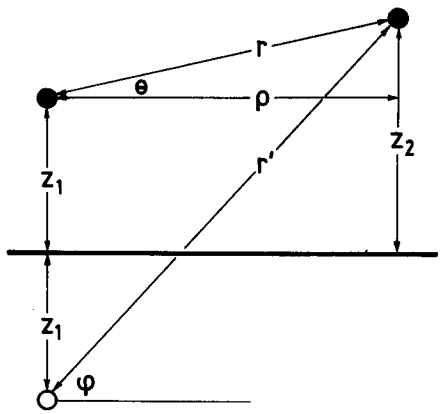

FIG. 1. Schematic representation of the coordinate system. The surface (located at $z = 0$) is indicated by the heavy solid line, and the two physisorbed atoms by the solid circles, while the "image" of one of the latter is shown as an open circle below the surface.

The periodicity of the semi-infinite solid allows the atom–surface potentials to be expressed as the Fourier expansions

$$V_{as}(\mathbf{r}_j) = V_{00}(z_j) + \sum_{\mathbf{G}}{}' V_{\mathbf{G}}(z_j)\exp(i\mathbf{G}\cdot\mathbf{R}_j)\,. \tag{10}$$

Here $\{\mathbf{G}\}$ are the reciprocal lattice vectors which correspond to the exposed surface of the substrate, and the prime on the sum indicates that the term with $\mathbf{G} = \mathbf{0}$ is to be excluded. $V_{00}(z)$ is the usual[25] lateral average of the atom–surface interaction, and the $V_{\mathbf{G}}(z)$ are the corrugation strength functions associated with the different reciprocal lattice vectors. Details regarding how the Fourier components of the potential are calculated will be presented in Sec. IV.

Of course, the precise values used for $\{\mathbf{G}\}$ are implicitly based on the assumptions that the substrate atoms are located at their assigned lattice sites, and that any displacements of the atoms from these equilibrium positions are quite small. However, at the temperatures of interest here, and indeed at any temperature where a significant amount of physisorption would occur, this assumption is certainly valid.

A two dimensional center of mass transformation is now introduced in order to separate the relative motion of the center of mass of the physisorbed atoms in directions parallel to the plane of the surface from the other degrees of freedom. Defining $M = m_1 + m_2$ and $\mu = m_1 m_2/M$, the new coordinates are

$$\mathbf{R} = (m_1\mathbf{R}_1 + m_2\mathbf{R}_2)/M\,, \tag{11}$$

$$\boldsymbol{\rho} = \mathbf{R}_1 - \mathbf{R}_2\,. \tag{12}$$

In terms of these coordinates Eq. (9) may be written as

$$H = H_1 + H_2 + H_M + H_\mu + W\,. \tag{13}$$

Here H_1 and H_2 are one-dimensional Hamiltonians which describe the motions of the physisorbed atoms normal to the surface:

$$H_j = -\frac{\hbar^2\partial^2}{2m_j\partial z_j^2} + V_{00}(z_j) \tag{14}$$

for $j = 1$ and 2. The term $H_M = -(\hbar^2/2M)\nabla_{\mathbf{R}}^2$ then governs the two-dimensional free particle translation of the center of mass of the two adatoms in directions parallel to the surface.

The fourth term in Eq. (13), H_μ, describes the relative motion of the adatom pair in directions parallel to the surface. However, in order to obtain a separable zeroth-order problem, the actual pair potential is simplified by introduction of a "frozen-z approximation" according to which the normal distance between each adatom and the surface is assumed to be fixed at its average value $\bar{z}_j$ ($j = 1,2$). As a result,

$$H_\mu = -\frac{\hbar^2}{2\mu}\nabla_{\boldsymbol{\rho}}^2 + V_{aa}\left[\sqrt{\rho^2 + (\bar{z}_1 - \bar{z}_2)^2}\right] + \Delta V_{aa}\left[\sqrt{\rho^2 + (\bar{z}_1 - \bar{z}_2)^2}\right]. \tag{15}$$

The first potential term appearing here is the (assumed known) free space interaction between the two atoms, while $\Delta V_{aa}\left[\sqrt{\rho^2 + (z_1^2 - z_2^2)}\right]$ arises from the surface modification of the atom–atom potential (see below).

The sum of the first four terms contributing to Eq. (13) defines the zeroth order Hamiltonian.

The last term in Eq. (13),

$$\begin{aligned} W = &\sum_{\mathbf{G}}{}' V_{\mathbf{G}}(z_1)e^{i\mathbf{G}\cdot(\mathbf{R} + \boldsymbol{\rho}m_2/M)} + \sum_{\mathbf{G}}{}' V_{\mathbf{G}}(\bar{z}_2)e^{i\mathbf{G}\cdot(\mathbf{R} - \boldsymbol{\rho}m_1/M)} \\ &+ \left\{V_{aa}\left[\sqrt{\rho^2 + (z_1 - z_2)^2}\right] - V_{aa}\left[\sqrt{\rho^2 + (\bar{z}_1 - \bar{z}_2)^2}\right]\right\} \\ &+ \left\{\Delta V_{aa}\left[\sqrt{\rho^2 + (z_1 - z_2)}\right] - \Delta V_{aa}\left[\sqrt{\rho^2 + (\bar{z}_1 - \bar{z}_2)^2}\right]\right\} \\ &+ \Delta V_{as}(\boldsymbol{\rho}, z_1, z_2) \end{aligned} \tag{16}$$

consists of all terms in Eq. (9) which contribute to coupling among the motions associated with the (separable) first four terms. It is of course W which drives the relaxation step, Eq. (7) of the reaction mechanism. The first pair of terms in Eq. (16) are the surface corrugation contributions to the atom–surface potential. The next two pairs of terms then account for the errors introduced into the surface mediated atom–atom interaction by the frozen-z approximation. The last term $\Delta V_{as}(\boldsymbol{\rho}; z_1, z_2)$ then represents the dependence of the atom–surface potential upon the atom–atom separation. It arises because the nature of the binding of the adatom to the surface changes as the adatoms approach very close to one another. However, it is argued below that this term is not important in the present problem.

The first four terms in Eq. (13) may be treated as independent Hamiltonians whose eigenvalues and eigenfunctions are readily determined using numerical or analytical techniques. Our procedure begins by substituting the laterally averaged atom–surface potential $V_{00}(z)$ into H_1 or H_2, and solves the resulting one-dimensional Schrödinger equation by standard techniques[21–23,26,27] to obtain the eigenvalues E_{n_1} and normalized wave functions $|n\rangle$ of the physisorption levels. The latter are then used to calculate the expectation values $\langle n|z_j|n\rangle = \bar{z}_j$ used in the frozen-z approximation.

The eigenfunctions of the two-dimensional center of mass translation Hamiltonian H_M are of course the normalized plane wave functions $\exp(i\mathbf{K}\cdot\mathbf{R})/L$ with eigenvalues $E_M = (\hbar K)^2/2M$. Here L is the length of the side of a box in which periodic boundary conditions have been applied.

In treating the adatom relative motion Hamiltonian H_μ, we first note that it is the introduction of the frozen-z approximation fixing the atoms at the normal distances $\bar{z}_j(n)$, which makes the problem separable. If the two adatoms are

in the same n state, their $\bar{z}_j$ values will be equal and the potential V_{aa} in Eq. (15) will have the usual form. If not, however, the difference between the $\bar{z}_j$ values has the effect of shifting the radial origin to large separations so that the effective pair potential V_{aa} remains finite at $\rho = 0$. This in turn usually means that this pair potential will be both totally attractive and weak, and hence that it will support few bound or quasibound levels which could participate in the recombination mechanism.

Since the potential terms in Eq. (15) depend only on the magnitude of ρ, and not on its orientation, the angular and radial components of its eigenfunctions are separable. The normalized angular eigenfunctions are $\exp(iJ\theta)/(2\pi)^{1/2}$, where the nonnegative integer J is the (two-dimensional) rotational quantum number. The equation governing the associated radial motion is then

$$-\frac{\hbar^2}{2\mu}\frac{d^2}{d\rho^2}\chi_{vJ} + \{[V_{aa} + \Delta V_{aa} + (J^2 - 1/4)\hbar^2/2\mu\rho^2 - E(v,J)]\}\chi_{vJ} = 0 . \quad (17)$$

The structure of this equation is identical to that for a diatomic molecule in three dimensions, except that the usual centrifugal strength coefficient $J(J+1)$ is replaced here by $(J^2 - 1/4)$. In practice, this change in the centrifugal term is responsible for most of the differences between the eigenvalues of the atom–atom potential in free space and on the surface.

Throughout the following, the labels m and s which identify the metastable and stable species of Eqs. (7) and (8) represent the sets of quantum numbers $\{n_1,n_2,v,J\}$ and $\{n_1',n_2',v',J'\}$, respectively. These indices are of course the physisorption quantum numbers of the constituent atoms, n_1 and n_2 or n_1' and n_2', and the internal vibration-rotation quantum numbers of the diatom pair, (v,J) and (v',J'). The zeroth order wave functions are therefore simple products of appropriate eigenfunction of the separable components, H_1, H_2, H_μ, and H_M of Eq. (13), while the relaxation step of Eq. (7) is simply an inelastic transition between two of these states, driven by the perturbation W of Eq. (16).

B. Surface modification of the atom–atom potential

The atom–atom interaction is of course affected by the presence of the substrate. The present work only considers its effect on the induced dipole–induced dipole term. However, in view of the distances involved and the size of the effects calculated here, it seems reasonable to assume that the effect of other such terms will also be negligible.

MacLachlan[24] has shown that when a pair of identical atoms are located above a surface, as shown in Fig. 1, the substrate contribution to the induced dipole–induced dipole interaction is

$$C_{s_1}[2 + 3\cos(2\theta) + 3\cos(2\phi)]/6(rr')^3 - C_{s_2}/(r')^6 . \quad (18)$$

The coefficients C_{sk} characterizing this interaction are given (in atomic units) by

$$C_{sk} = (3/\pi)\int_0^\infty d\omega \left[\frac{\epsilon(i\omega) - 1}{\epsilon(i\omega) + 1}\right][\alpha(i\omega)]^k , \quad (19)$$

where $\epsilon(\omega)$ is the dielectric response of the substrate and $\alpha(\omega)$ the free space polarizability of the adatoms. Note that both the polarizability of the atom and the dielectric response of the substrate are evaluated at complex frequencies. One drawback of the MacLachlan expression (18) is that its first term diverges as the adatom–adatom separation r approaches zero. This should not be surprising, since this expression was obtained from an asymptotic expansion of a perturbation series, and the divergence arises when this result is used beyond its region of validity. In order to suppress this singularity, the correction function $\Delta V_{aa}\left[\sqrt{\rho^2 + (z_1^2 - z_2^2)}\right]$ is defined as a product of the MacLachlan term (18) times a damping function $D(r)$ determined by fitting the directly calculated H_3 damping function of O'Shea and Meath[28] to a simple functional form.[29]

C. The metastable state equilibrium constant K_e^m

For any given metastable state m, the equilibrium constant K_e^m can be calculated using elementary statistical mechanics. In particular,

$$K_e^m = [X_2^*(m)]/[X]^2 = \{[Q_{X_2}^*(m)]/L^2\}/\{Q_X/L^2\}^2 , \quad (20)$$

where $[P]$ denotes the equilibrium number of atoms or molecules of species P per unit area, Q is the partition function for species P, and L is the reference length which normalizes the center of mass wave function defined by H_M. The partition function for the adatoms X is a product of a term associated with each degree of freedom of the atom; one for its free translational motion in two dimensions (parallel to the surface), times a sum over the bound states $|n\rangle$ of the atom–surface potential $V_{00}(z)$:

$$Q_X/L^2 = (m_1/2\pi\beta\hbar^2)\sum_n \exp\{-\beta E_n\} , \quad (21)$$

where $\beta = 1/(k_b T)$ and k_b is Boltzmann's constant.

The partition function for the metastable species $X_2^*(m)$ is obtained in a similar fashion. This species is formed from atoms in physisorption levels n_1 and n_2, has internal energy $E(v,J)$, and has a two-dimensional center of mass translational energy (for motion parallel to the surface) of $E = (\hbar K)^2/2M$. As a result,

$$Q_{X_2}^*(m)/L^2 = [M(2 - \delta_{J,0})/2\pi\beta\hbar^2] \times \exp\{-\beta[E_{n_1} + E_{n_2} + E(v,J)]\}, \quad (22)$$

where $(2 - \delta_{J,0})$ is the rotational degeneracy factor, and we have summed over all possible center of mass translational energies. Substituting Eqs. (21) and (22) into Eq. (20) then yields the desired expression for the equilibrium constant for metastable species m:

$$K_e^m = (2\pi\beta\hbar^2 M/m_1^2)(2 - \delta_{J,0}) \times \exp\{-\beta[E_{n_1} + E_{n_2} + E(v,J)]\} \Big/ \left[\sum_{n_1}\exp(-\beta E_{n_1})\right]^2 . \quad (23)$$

D. The relaxation step rate constant $k_r^{m,s}$

Since the relaxation step in the recombination mechanism is first order, and both the initial and final states involve

a continuum, use of Fermi's Golden Rule[30] yields the reaction rate expression

$$k_r^{m,s}(t) = (2/\hbar) \sum_{\mathbf{K}\mathbf{K}'} P(\mathbf{K},T) |\langle s,\mathbf{K}'|W|m,\mathbf{K}\rangle| \times (E_s - E_m)^{-1} \sin[(E_s - E_m)t/\hbar] , \quad (24)$$

where t is the time since the metastable state $|m,\mathbf{K}\rangle$ was formed and (as indicated at the end of Sec. III A) the wave functions $|m,\mathbf{K}\rangle$ and $|s,\mathbf{K}'\rangle$ are eigenfunctions of the zeroth order Hamiltonian $H_0 = H_1 + H_2 + H_\mu + H_M$. Here,

$$P(\mathbf{K},T) = (L^2 M/2\pi\beta\hbar^2)\exp(-\beta\hbar^2 K^2/2M) \quad (25)$$

is simply the probability that a center of mass translational state with wave vector $\mathbf{K}$ will be thermally populated.

In the results which follow, the transition matrix elements appearing in Eq. (24) were calculated while ignoring all but the first pair of terms in the perturbation W of Eq. (16). Since they incorporate only relatively weak coupling between ρ and the normal coordinate $\bar{z}_j$ (see below), the relaxation step of Eq. (7) effectively is assumed to proceed mainly by conversion of the internal vibration-rotation energy of the metastable pair into two-dimensional center of mass translational energy.

The neglected terms from W couple the internal vibration-rotation motion to motion along the physisorption coordinates z_j. While their omission is certainly expedient, it can in fact be strongly justified. In particular, consider the second and third pairs of terms, those which correct for the Hamiltonian of Eq. (15). For the latter (third) pair, this approximation can introduce negligible error, since the corresponding potential term ΔV_{aa} is itself very small (see Sec. IV B below). More generally, use of this approximation is justified whenever the average displacements of the atoms from their mean positions $\bar{z}_j$ are small compared to the adatom–adatom separation itself. For the metastable states considered below, this separation is typically five times larger than the amplitudes of the motion normal to the surface. Thus, coupling due to the frozen-z approximation should not be large.

The last term in the definition of W represents the change in the potential governing their binding to the surface as the two adatoms come together and distort one another's electronic distributions. However, for both the bound and metastable states considered below, the adatom–adatom bond length is typically ~ 2.7 Å, which is 3.5 times the equilibrium bond length. At these distances it seems unlikely that the distortion of the electron distributions would significantly affect the surface binding forces.

Retaining only the first pair of terms in the perturbation W of Eq. (16), an exercise in algebra yields the required matrix elements:

$$\langle s,\mathbf{K}'|W|m,\mathbf{K}\rangle = \sum_{\mathbf{G},n_1,n_2}{}' i^{(J-J')} \times \{\delta_{n_1 n_1'}\langle V_{\mathbf{G}}\rangle_{n_2}^{n_2'} + \delta_{n_2,n_2'}\langle V_{\mathbf{G}}\rangle_{n_1}^{n_1'}\exp[i(J-J')\pi]\} \times f(v,J,v',J'|\mathbf{G}|)\times\delta_{\mathbf{K}+\mathbf{G},\mathbf{K}'} , \quad (26)$$

where δ is the Kronecker delta, and $\mathbf{G}$ is a reciprocal lattice vector whose presence is required to enforce conservation of momentum parallel to the surface. In this expression the quantity

$$\langle V_{\mathbf{G}}\rangle_{n_1}^{n_1'} = \langle n_1'|V_{\mathbf{G}}(z)|n_1\rangle \quad (27)$$

is a matrix element of the corrugation strength function corresponding to reciprocal lattice vector $\mathbf{G}$, and

$$f(v,J,v',J'|\mathbf{G}|) = \int_0^\infty d\rho\, \chi_{v'J'}^*(\rho)\chi_{vJ}(\rho)J_{|J-J'|}(G\rho/2) \quad (28)$$

an analogous one-dimensional matrix element between eigenfunctions of Eq. (17) for the stable and metastable species, where $J_n(x)$ is the regular Bessel function of order n.[31] Note that if both atoms are in the same physisorption state (i.e., $n_1 = n_2$) and undergo the same (lack of) transition (such that $n_1' = n_2'$), the above result yields the selection rule $J - J' =$ even.

E. The overall rate constant

At this point, all the ingredients necessary for calculating the overall rate constant are available. However, in order to simplify the form of the final expression so as to make its structure more apparent, it is convenient to now introduce a couple of simplifying approximations which have no effect on the numerical predictions presented below. The first of these is based on the fact that at sufficiently low temperatures, Eq. (23) shows that only the physisorption ground state will be significantly populated: as a result, it is reasonable to set $n_1 = n_2$. The second is that the small magnitude of the matrix elements $\langle V_{\mathbf{G}}\rangle_{n_1}^{n_1'}$ for $n_1 \neq n_1'$ means that only the diagonal terms $n_1 = n_1'$, need be retained in the sums of Eq. (26). Subject to these approximations, substitution of Eqs. (25) and (26) into Eq. (24) yields

$$k_r^{m,s}(t) = (4\pi\beta\hbar/L^2 m_1)[1 + (-1)^{J-J'}] \sum_{\substack{\mathbf{K}\mathbf{K}'\\ \mathbf{G}\mathbf{G}'}} \langle V_{\mathbf{G}}\rangle_0^0\langle V_{\mathbf{G}'}\rangle_0^0 f(v,J,v',J'|\mathbf{G}|)f(v,J,v',J'|\mathbf{G}'|) \times \exp(-\beta\hbar^2 K^2/2M)\sin\{[\hbar^2 K'^2/2M - \hbar^2 K^2/2M + E(v',J') - E(v,J)]t/\hbar\} \times [\hbar^2 K'^2/2M - \hbar^2 K^2/2M + E(v',J') - E(v,J)]^{-1}\delta_{\mathbf{K}+\mathbf{G},\mathbf{K}'}\delta_{\mathbf{K}+\mathbf{G}',\mathbf{K}'} . \quad (29)$$

The presence of the Kornecker deltas in Eq. (29) trivially collapses the sums over $\mathbf{K}'$ and $\mathbf{G}'$. Converting the sum over $\mathbf{K}$ into an integral and using the properties of the Dirac delta function appropriate to the limit where $t \to \infty$, Eq. (29) then becomes

$$k_r^{m,s} = (\beta\hbar/m_1)[1+(-1)^{J-J'}]\sum_{\mathbf{G}}[\langle V_{\mathbf{G}}\rangle_0^0 f(v,J,v',J'|G)]^2$$

$$\times\int_0^\infty dK\,K\int_0^{2\pi} d\theta\exp(-\beta\hbar^2K^2/2M)\delta[\hbar^2G^2/2M+\hbar GK\cos(\theta)/M+E(v',J')-E(v,J)]\,, \tag{30}$$

where θ is the angle between the directions of **K** and **G**. After using the delta function to perform the integral over the magnitude of K, the final integral over θ can be brought into a standard form[33] by the transformation $x^{-1}=\cos^2(\theta)$, yielding:

$$k_r^{m,s} = [4(\pi m_1\beta)/\hbar^2][1+(-1)^{J-J'}]\sum_{\mathbf{G}}[\langle V_{\mathbf{G}}\rangle_0^0 f(v,J,v',J'|\mathbf{G}|)]^2$$

$$\times\exp\{-(\beta M/2\hbar^2G^2)[E(v,J)-E(v',J')-\hbar^2G^2/2M]^2\}\,. \tag{31}$$

Substitution of Eqs. (23) and (31) into Eq. (8) then yields the desired expression for the overall rate constant of Eq. (6):

$$k = \sum_{vJv'J'}{}' K_e^{vJ}k_r^{vJ,v'J'}(2-\delta_{J',0})/[1+k_r^{vJ,v'J'}/k_b^{vJ}]\,. \tag{32}$$

The prime on the sum here indicates that only states for which $E(v',J')<0$ and $E(v,J)>0$ are to be included, while the factor $(2-\delta_{J',0})$ arises from the degeneracy of the final rotational state. Note that for the sake of explicitness, we have made the cosmetic replacement of (v,J) for m and (v',J') for s.

F. Selection of participating metastable states

At low temperatures, the number of metastable orbiting-resonance states (v,J) which contribute significantly to the sum in Eq. (32) is rather small. The restrictions governing their selection arise from two sources; the first is the nature of the metastable states themselves while the second is thermodynamic. We discuss them in turn, beginning with the former.

We first note that the back reaction rate constants k_b^m of Eq. (2) are directly proportional to the tunneling predissociation widths of the corresponding metastable levels; in particular:

$$k_b^m = 2\pi c/\Gamma\,, \tag{33}$$

where Γ is the level width in cm^{-1} and c the speed of light. Since the magnitudes of the other factors (K_e^m and $k_r^{m,s}$) in the rate constant expression do not depend on the level widths, Eq. (32) [or Eq. (8)] shows that if the rate constant is sufficiently small, the corresponding state (v,J) will contribute little to the overall reaction rate. As a result, the narrower orbiting resonance levels can be omitted from the sum over v and J in Eq. (32). The physical reason for this selectivity is simply the fact that if the width of a level is very small, the probability of tunneling through the potential barrier at that energy is sufficiently small that a measurable population will never accumulate.

The thermodynamic restrictions on the choice of participating levels arise simply from Boltzmann considerations. Consider the set of rotational sublevels associated with a given value of the diatom vibrational quantum number v. As the energies of these levels increase with increasing J, so do the corresponding level widths. Thus, while the narrower (lower energy) resonances are excluded from participation by the considerations outlined above, the broadest (highest energy) ones are discriminated against by the Boltzmann factors incorporated in the equilibrium constants K_e^m. In practice this means that only states which lie near relatively low potential barrier maxima (i.e., those corresponding to relatively small values of the diatom rotational quantum number J) can contribute significantly to the overall reaction rate constant. Since the energy associated with a vibration-rotation level lying near a barrier maximum increases rapidly with decreasing vibrational quantum number, this means that (as was found in the gas phase case[18]) only resonances associated with the highest vibrational levels can contribute significantly to this reaction mechanism.

Although the above restrictions may appear to be somewhat nebulous, in practice it is relatively easy to identify the important metastable orbiting resonance states, and the number of initial and final states which enter the summation is small. Note, however, that the recipe outlined above tends to underestimate the overall reaction rate constant since it neglects the contributions of some of the less favored intermediate states.

IV. APPLICATION TO HYDROGEN RECOMBINATION ON XENON

This section presents predictions of the rate constants implied by our model for the case of atomic hydrogen or deuterium recombining on a xenon substrate. In addition to inherent interest in hydrogen recombination per se, the motivation for this choice is twofold. First of all, the model requires that the recombining adatoms be physisorbed, and not chemisorbed, so that they may be free to move about on the surface. To achieve this requires a rather inert substrate, such as that provided by an inert gas crystal. Their relatively large zero point energy for motion normal to the surface and relatively long de Broglie wavelength for motion parallel to the surface make hydrogenic atoms a particularly good choice in this regard too. The second reason for this choice is the fact that the hydrogen–xenon pair potential is well known.[34] This means that the model is completely specified once the surface plane is chosen.

Within the above model, we have determined the overall recombination rate on both the (111) and (100) planes of crystalline xenon. The (111) plane is densely packed and highly corrugated, whereas the (100) plane is more loosely

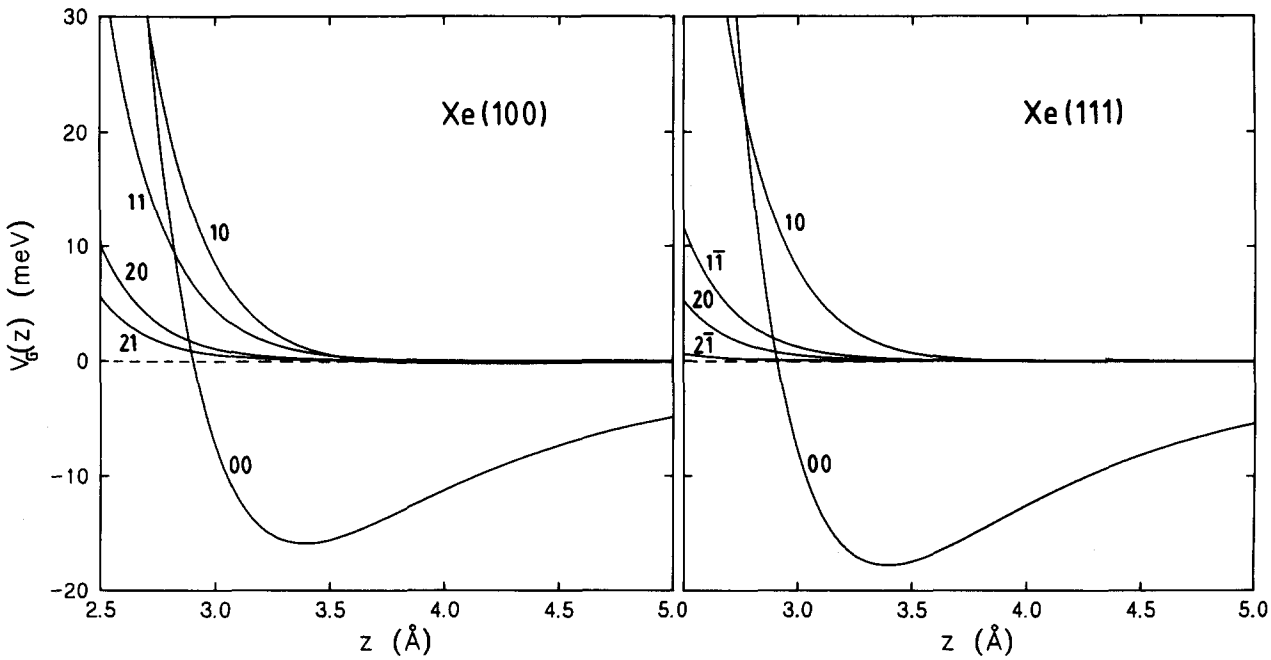

FIG. 2. Fourier components of the atom–surface potential as a function of normal separation z, for hydrogen interacting with either Xe(100) or Xe(111). The Fourier components are labeled MN with $\mathbf{G} = M\mathbf{g}_1 + N\mathbf{g}_2$ where $\mathbf{g}_1$ and $\mathbf{g}_2$ are the primitive reciprocal lattice vectors appropriate to the exposed crystal facet.

packed and has relatively less corrugation. We use a direct space lattice constant of 6.2 Å for the solid xenon, and ignore its dependence on temperature. This is possible because over the temperature range of interest, the effect of substrate expansion or contraction is negligible. In particular, the change in bulk modulus over this range (4–10 K) suggests that the direct space lattice vectors would change by less than 1%.

The above choice of lattice constant implies that a (111) cell has unit lattice vectors of magnitude $6.2/\sqrt{2}$ Å inclined at angles of 60° relative to each other. Similarly, for the (100) face, the lattice vectors have the same magnitude, but are mutually orthogonal. Note too that the (111) crystal face is sixfold degenerate while the (100) plane is fourfold degenerate.

A. The atom–surface interaction potential

The Fourier components of the atom–surface potential are calculated using the method of Steele.[25] In particular, the Fourier components of the l th layer, whose normal distance from the adatom is $z_l = z + ld$, where d is the interlayer spacing, is given by

$$V_{l,\mathbf{G}}(z_l) = (2\pi/a_c)\int_0^\infty dR\, RJ_0(GR)U(z_l,R)\,, \tag{34}$$

where a_c is the area of the corresponding direct space unit cell, G the magnitude of the appropriate lattice vector, and U the atom–atom pair potential. For the (111) face $d = 6.2/\sqrt{3}$ Å, and for the (100) face $d = 3.1$ Å. One then merely sums the contribution from each layer to obtain the overall Fourier components $V_{\mathbf{G}}$ of Eq. (10).

Of course the above procedure assumes that the atoms of the substrate are at their equilibrium positions, and ignores thermal displacements due to phonons. Allowing for the presence of phonons would have required the inclusion of an additional term in each layer potential. These terms would have the structure of Eq. (34), with the replacement of U by $\boldsymbol{\xi}\cdot\nabla U$ for U, where $\boldsymbol{\xi}$ is the displacement of an atom from its equilibrium site position. However, such effects are expected to be small at the temperatures of interest here, and their inclusion is beyond the scope of the present work.

On combining the above lattice constants and interlayer separations with the HFD-1 hydrogen–xenon pair potential of Douketis *et al.*,[34] the Fourier components were evaluated in the manner described above. It was found that a 21 layer

TABLE I. Energies E_n (in cm^{-1}) and expectation values of z, $\bar{z}_n$ (in Å) for the first four physisorption bound states of H or D on Xe(100) and Xe(111).

	H/Xe(111)		H/Xe(100)		D/Xe(111)		D/Xe(100)	
n	E_n	$\langle n\|z\|n\rangle$	E_n	$\langle n\|z\|n\rangle$	E_n	$\langle n\|z\|n\rangle$	E_n	$\langle n\|z\|n\rangle$
0	− 85.331	3.760	− 73.990	3.782	− 100.390	3.634	− 87.917	3.646
1	− 22.296	5.061	− 17.710	5.233	− 42.801	4.342	− 35.536	4.422
2	− 3.376	8.301	− 2.345	9.037	− 14.492	5.614	− 11.204	5.861
3	− 0.187	19.786	− 0.098	23.479	− 3.659	8.075	− 2.565	8.752

TABLE II. Values (in cm^{-1}) of the diagonal matrix elements $\langle V_G \rangle_0^0$ associated with the four lowest-order reciprocal lattice vectors, for H and D on Xe(100) and Xe(111).

G_n	H/Xe(111)	H/Xe(100)	D/Xe(111)	D/Xe(100)
1	8.6510	8.0018	9.2043	8.4792
2	1.3990	5.2240	1.4703	5.6015
3	0.0484	1.2308	0.5614	1.3002
4	0.0202	0.6041	0.0484	0.6307

sum was fully converged. Figure 2 shows plots of the first few Fourier components for each of the crystal faces considered. We remark in passing that the resulting lateral averaged surface potentials V_{00} are in reasonable agreement with the recently proposed "universal" potential of Vidali *et al.*[35]

The properties of the adatom–surface potential required in the present calculation are summarized in Tables I and II. These include the energy eigenvalues of the one dimensional laterally averaged potential V_{00} for each isotope on each face of the crystal, and the expectation values of z for each of these levels. These eigenvalues were generated by numerical solution of the Schrödinger equation (14) using standard techniques,[23,26,27] and the wave functions thus obtained were used to generate the expectation values $\langle V_G \rangle_0^0$ defined by Eq. (27), together with the average $\bar{z}_j$ values.

B. The adatom–adatom interaction

The other ingredient required by the present model is the adatom–adatom interaction. For the free space potential, we have used the Bishop–Shih potentials[36] for H_2 and D_2. Calculation of the damped McLachlan potential requires knowledge of the dielectric response of xenon and the polarizability of hydrogen. To obtain the dielectric response of xenon (for which we know of no existing data), we employed the Clausius–Mossotti relationship linking polarizability with dielectric response. The polarizabilities were obtained from Tang *et al.*,[37] and Eq. (19) was then used to obtain $C_{S1} = 1.9207$ and $C_{S2} = 0.6180$, both in atomic units. For the appropriate values of $\bar{z}_1$ and $\bar{z}_2$ (see Table I), the effective adatom pair potential $[V_{aa} + \Delta V_{aa}]$ of Eq. (17) is then fully defined. In general, the damped McLachlan interaction was found to be small at all distances, approximately parts in 10^{-5} compared to the Bishop–Shih potential.

Solution of the eigenvalue problem defined by Eq. (17) yields the manifold of metastable states whose properties are summarized in Tables III and IV. The difference between the properties of these states and those of the usual free space results may be understood in the following way. Since the McLachlin term is so weak, the centrifugally distorted potential in two dimensions is effectively equal to the corresponding three dimensional gas phase potential minus a term of the form $(J + 1/4)\hbar^2/2\mu\rho^2$. First-order perturbation theory then shows that the energy of a two dimensional state labeled by the indices (v,J) is related to that of the corresponding free space level by the expression

$$E^{2D}(v,J) = E^{3D}(v,J) - B_v^{3D}(J + 1/4)\,. \tag{35}$$

Here B_v^{3D} is the usual gas phase inertial rotational constant. This shows that the two dimensional levels are more deeply bound than the corresponding three-dimensional ones. Tables III and IV list the energies (relative to the dissociation limit) and widths of the metastable states which could be important in the present context for H and D physisorbed on the (100) and (111) crystal faces of xenon.

C. Results

At each temperature of interest, the relaxation rate constant of Eq. (31) was evaluated for each of the metastable states listed in Tables III and IV, subject to the $J - J' =$ even selection rule and the two following restrictions. Transitions were considered to all possible stable final states for which the argument of the exponential in Eq. (31) was less than 50, and for which the G vector labeling the transition was less than fourth order. This last criterion reflects the rapid decrease of the $\langle V_G \rangle_0^0$ matrix elements with the magnitude of G. Note that this exponential factor arises simply from the Boltzmann distribution of translational states on the surface; the population factor for the (v,J) states is included in the equilibrium constant K_e^m. For a range of typical metastable and final states, illustrative values of these rate constants are shown in Table V.

The overall rate constant of Eq. (32) is now easily evaluated; results for $T = 4$ and 10 K are listed in Table VI. For H atoms on either crystal face, the overall rate is dominated by recombination via the metastable level $v = 14$, $J = 5$. From

TABLE III. Energies $E(v,J)$ and widths Γ (both in cm^{-1}) of the important metastable states for H_2 on Xe(100) and Xe(111); the zero of energy is the H_2 dissociation limit.

		H/Xe(111)		H/Xe(100)	
v	J	$E(v,J)$	Γ	$E(v,J)$	Γ
14	5	24.41	4.37	24.40	4.37
13	8	23.03	0.38×10^{-3}	23.02	0.38×10^{-3}
13	9	145.60	19.96	145.59	19.95
12	11	107.74	0.01	107.73	0.01
12	12	305.89	25.84	305.87	25.83
11	13	33.40	0.46×10^{-11}	33.39	0.45×10^{-11}
11	14	347.62	1.37	347.61	1.37
8	19	20.84	0.21×10^{-29}	20.83	0.21×10^{-29}
7	21	156.08	0.54×10^{-17}	156.06	0.53×10^{-17}
4	26	107.59	0.70×10^{-33}	107.52	0.70×10^{-31}

TABLE IV. Energies $E(v,J)$ and widths Γ (both in cm^{-1}) of the important metastable states for D_2 on Xe(100) and Xe(111); the zero of energy is the D_2 dissociation limit.

		D/Xe(111)		D/Xe(100)	
v	J	$E(v,J)$	Γ	$E(v,J)$	Γ
20	7	23.23	1.42	23.23	1.42
19	11	87.43	3.18	87.42	3.18
19	10	15.10	0.41×10^{-5}	15.09	0.40×10^{-5}
18	14	150.80	1.21	150.79	1.21
18	13	33.65	0.23×10^{-6}	33.64	0.22×10^{-6}
17	17	271.60	2.78	271.56	2.78
17	16	117.17	0.17×10^{-3}	117.17	0.17×10^{-3}
16	19	282.81	0.39×10^{-1}	282.80	0.39×10^{-1}
16	18	68.89	0.21×10^{-10}	68.88	0.20×10^{-10}
15	21	294.13	0.27×10^{-10}	294.11	0.27×10^{-3}
15	20	25.57	0.12×10^{-22}	25.56	0.12×10^{-22}
14	23	320.34	0.30×10^{-5}	320.33	0.30×10^{-5}
13	24	0.910	a	0.90	a
12	26	35.00	a	34.99	a
11	28	106.77	0.27×10^{-26}	106.72	0.27×10^{-26}
10	30	219.44	0.16×10^{-21}	219.43	0.16×10^{-21}
7	35	173.00	a	172.99	a
4	40	305.11	a	305.09	a
2	43	220.58	a	220.57	a
0	40	185.09	a	185.09	a

[a] Width less than 10^{-35} cm^{-1}.

the viewpoint of population alone, this result may seem somewhat surprising, as the $v=13, J=8$ level lies at nearly the same energy and (see Table III) its relaxation rate constant $k_r^{m,s}$ is relatively large. However, the $v=13, J=8$ level has a width which is four orders of magnitude smaller than that of $v=14$, $J=5$ (see Table III), so, its contribution is reduced by the presence of the k_b^m of Eq. (33) in the denominator of Eq. (32).

An analogous situation arises for deuterium. In this case the overall rate is dominated by recombination via the $v=20$, $J=7$ level, despite the fact that the $v=19$, $J=10$ state is thermally preferred. It is interesting to note that neglect of the role of the back reaction rate constant k_b^m (i.e., the level width) which the steady state approximation places in the denominator of Eq. (32) would have yielded overall rate constants for both isotopes some two orders of magnitude larger than the results reported in Table VI.

V. DISCUSSION AND CONCLUSIONS

In order to obtain a better feeling for the magnitudes of the separate constants, it may be convenient to think of them in terms of reaction half-lives. Since the overall reaction is second order [see Eq. (6)], an initial concentration of C_0 at time $t=0$ would yield a half-life of $t_{1/2}=2/(C_0k)$. For an initial concentration of 1 H (or D) atom per 5 unit cells, the resulting predicted half-lives are given in Table VII. These half-lifes are small, so this recombination would occur rapidly.

An alternative view of these results is to express them as an effective reaction diameter $D=k(T)/v(m,T)$, where $v(m,T)$ is the two dimensional average velocity of an atom of mass m on the surface. From elementary statistical thermodynamics, $v(m,T)=(\pi k_b T/2m)^{1/2}$. Combining this average velocity with the calculated rate constants then yields the reaction diameters listed in Table VII. The square of this

TABLE V. Illustrative values of the relaxation rate constants $k_r^{m,s}$ and the ratio $k_r^{m,s}/[1+k_r^{m,s}/k_b^m]$ (both in units of 10^{10}/s) at $T=4$ and 10 K, for H atoms recombining on Xe(111).

					$T=4$ K		$T=10$ K	
v	J	v'	J'	ΔE	$k_r^{m,s}$	$k_r^{m,s}/[1+k_r^{m,s}/k_b^m]$	$k_r^{m,s}$	$k_r^{m,s}/[1+k_r^{m,s}/k_b^m]$
14	5	14	3	95.76	0.497	0.494	1.099	1.086
		10	15	49.24	7.921×10^{-8}	7.921×10^{-8}	1.466×10^{-7}	1.466×10^{-7}
		14	1	159.86	9.080×10^{-3}	9.079×10^{-3}	0.131	0.130
		13	7	145.52	3.008×10^{-3}	3.008×10^{-3}	0.011	0.011
13	8	14	2	133.39	0.3989×10^{-2}	6.137×10^{-3}	0.97	6.752×10^{-3}
		14	4	46.22	7.881	7.246×10^{-3}	13.156	7.249×10^{-3}
		14	0	167.12	6.298×10^{-4}	5.795×10^{-4}	7.604×10^{-4}	6.883×10^{-4}
		12	10	154.86	3.473×10^{-3}	2.349×10^{-3}	0.053	6.387×10^{-3}
		13	6	290.94	6.760×10^{-8}	6.760×10^{-8}	1.338×10^{-5}	1.336×10^{-5}
		11	12	340.69	2.113×10^{-12}	2.113×10^{-12}	7.611×10^{-9}	7.611×10^{-9}

TABLE VI. Calculated overall recombination rate constants (in units 10^8 Å/molecule s) for H and D on Xe(100) or Xe(111), at 4 and 10 K.

	Xe(111)		Xe(100)	
T/K	H	D	H	D
4	4.96	27.27	2.57	35.93
10	906.25	1684.07	1761.79	2040.50

reaction diameter (times π) would be the analog of a three-dimensional reaction cross section; these values would clearly be quite small.

It is important to note that the recombination rate is not particularly sensitive to the choice of crystal face. For hydrogen, the recombination rate is roughly a factor of 2 slower on the open (100) face than on the dense packed (111) face. The results in Table II show that this is largely due to the smaller strength of the corrugation and the degeneracy in the former case.

Another interesting result is the fact that the D atom recombination rate is *faster* than that for H atoms, on either crystal face. This is in sharp contrast to the case for either "normal" thermal reactions, where the smaller zero point energy of a heavy isotope would make its activation energy higher, or for low temperature tunneling-dominated reactions where the light isotope would again react much more rapidly.[38]

The most obvious "apparent" explanation for this is simply that since the heavier isotope has a larger density of internal vibration-rotation states, there will be a larger number of contributing metastable D_2 levels, and they will lie at relatively lower energies, and hence be more heavily populated. However, while these considerations would in general tend to favor the heavy isotope, closer scrutiny shows that they have at most a minor effect here. In particular, it was pointed out above that at the temperatures of interest, a single metastable state was responsible for almost all of the recombination for each isotope, so the *number* of contributing states per se does not play a role. At the same time, examination of the results in Tables III and IV shows that the energies of the dominant metastable states are almost exactly the same, so that although the D_2 level lies ~ 1.2 cm^{-1} lower than that for H_2, this energy difference alone is not nearly enough to explain the observed isotope effect.

In this particular case then, the isotope effect seems to be due to a combination of this small energy difference with the explicit mass factors which appear at various places in the equilibrium and rate constant expressions, and with the density of states effect which makes the energy difference $[E(v,J) - E(v',J')]$ in the exponent of Eq. (31) smaller for D_2 than for H_2.

Finally, we wish to delineate areas in which the model needs to be improved. The first of these is the retention of the remaining terms of Eq. (16) in the calculation of the rate constants $k_r^{m,s}$. Clearly, this can only increase the magnitude of the matrix elements, and hence the rate at which the molecule is stabilized. This in turn will lead to an increase in the size of the overall recombination rate constant. A second extension of the model involves the removal of the frozen-z approximation.[39] This will allow the atoms to change their physisorption state and should lead to interesting effects, such as desorption. Another extension of the model is to improve the estimate of the stabilization rate $k_r^{m,s}$ given by Fermi's Golden Rule.

In addition to the above improvements in its implementation, we should also point out areas in which the present model needs to be extended so as to better approach the "real world." A first improvement of this type would be a relaxation of the rigid surface approximation. For a solid at any finite temperature, both bulk and surface phonons are present. Since the atom–surface potential is represented as a Fourier expansion about the equilibrium configuration, their presence will add displacement-dependent contributions to all of the Fourier components. The phonon field will then also be able to exchange energy with the atoms and/or molecules physisorbed to the surface. Another desirable extension of the model would be to also allow for collisional relaxation of the metastable species $X_2^*(m)$.

It would also be interesting to apply the present model to recombination of other species, and on other surfaces. A surface of particular interest would be liquid helium since this is the surface coating of the containers in which spin-polarized hydrogen is stored in current experiments.[15,16] The possibility of hydrogen atoms recombining on the triplet state potential would also be interesting to consider; although this potential supports no bound states in the gas phase, the different centrifugal potential for physisorbed atoms moving in two dimensions might allow this to occur.

In conclusion we have proposed a mechanism by which physisorbed atoms can recombine to form molecules. The mechanism we propose is an analog of the gas phase orbiting-resonance model.[18] Within the approximations we have employed, the metastable molecules are stabilized by trading internal vibration-rotation energy for increased center of mass translational energy. For a given adatom we find that the recombination rate is not extremely sensitive to the ex-

TABLE VII. Calculated half-lives $t_{1/2}$(ns) and effective collision diameter σ(Å) for an assumed concentration of 1 H or D atom per 5 unit cells, on Xe(100) or Xe(111), at $T = 4$ or 10 K.

	Xe(111)				Xe(100)			
	H		D		H		D	
T/K	$t_{1/2}$	σ	$t_{1/2}$	σ	$t_{1/2}$	σ	$t_{1/2}$	σ
4	335.58	2.08×10^{-4}	61.03	2.39×10^{-3}	747.86	1.60×10^{-4}	53.49	3.15×10^{-1}
10	1.83	3.55×10^{-2}	0.98	9.35×10^{-2}	1.09	6.92×10^{-2}	0.94	1.13×10^{-1}

posed crystal face of the substrate. We have also explored the dependence of the overall recombination rate upon the mass of the recombining atom and find that the heavier isotope has a *larger* overall recombination rate.

In general, the effects omitted from the present calculation are such that the overall recombination rate constants obtained here should be lower bounds to the actual recombination rate. In particular, recombination may also occur by other mechanisms, and we have as yet no basis for assuming that any one mechanism is dominant. Nevertheless, the results obtained here should still be of lasting value since they were generated from a well defined model based upon accurately known interactions using a minimal number of approximations.

ACKNOWLEDGMENTS

We would like to thank G. Scoles and M. Vax for the numerous enlightening and stimulating conversations. This work was supported by an operating grant from the Natural Sciences and Engineering Research Council of Canada.

[1]G. E. Gdowski, J. A. Fair, and R. J. Madix, Surf. Sci. **127**, 541 (1983).
[2]G. E. Gdowski and R. J. Madix, Surf. Sci. **115**, 524 (1982).
[3]G. B. Demidovitch, V. F. Kislev, H. H. LeJnev, and O. V. Nikiline, J. Chim. Phys. **64**, 1072 (1972).
[4]D. R. Olander, W. Sickhaus, R. Jones, and J. A. Schwarz, J. Chem. Phys. **57**, 408 (1972).
[5]R. Jones, D. E. Olander, W. Sickhaus, and J. A. Schwarz, J. Chem. Phys. **57**, 423 (1978).
[6]G. W. Rubloff, H. Luth, J. E. Demuth, and W. D. Grobman, J. Catal. **53**, 423 (1978).
[7]K. Bhattacharya, J. Chem. Soc. Faraday Trans. 1 **76**, 126 (1980).
[8]J. E. Demuth, H. Ibach, and S. Lehwald, Phys. Rev. Lett. **40**, 1044 (1978).
[9]T. S. Wittrig, P. D. Szuromi, and W. H. Weinberg, Surf. Sci. **116**, 414 (1982).
[10]T. E. Madey and J. T. Yates, Surf. Sci. **76**, 397 (1978).
[11]H.-J. Glas and H. G. Weber, Z. Phys. A **284**, 253 (1978).
[12]D. W. Trainor, D. O. Ham, and F. Kaufman, J. Chem. Phys. **58**, 4599 (1973).
[13]L. P. Walkauskas and F. Kaufman, J. Chem. Phys. **64**, 3885 (1976).
[14]D. N. Mitchell and D. J. LeRoy, J. Chem. Phys. **67**, 1042 (1977).
[15]R. Sprik, J. T. M. Walraven and I. F. Silvera, Phys. Rev. Lett. **51**, 479 (1983).
[16]H. F. Hess, D. A. Bell, G. P. Kochanski, R. W. Cline, D. Kleppner, and J. T. Greytak, Phys. Rev. Lett. **51**, 483 (1983).
[17]D. J. Hollenbach, Ph.D. thesis, Cornell University, 1969 (unpublished).
[18]R. E. Roberts, R. B. Bernstein, and C. F. Curtiss, J. Chem. Phys. **50**, 5163 (1969).
[19]A. W. Yu and H. W. Pritchard, J. Phys. Chem. **83**, 134 (1979).
[20]P. W. Atkins, *Physical Chemistry* (Freeman, San Francisco, 1978), p. 695.
[21]R. J. LeRoy and R. B. Bernstein, J. Chem. Phys. **54**, 5114 (1971).
[22]R. J. LeRoy and W.-K. Liu, J. Chem. Phys. **69**, 3622 (1978).
[23]A FORTRAN program for calculating bound and quasibound levels may be obtained from one of the authors on request: R. J. LeRoy, University of Waterloo Chemical Physics Research Report CP-230R (1983).
[24]A. D. McLachlan, Mol. Phys. **7**, 381 (1964).
[25]W. A. Steele, Surf. Sci. **36**, 317 (1973).
[26]J. W. Cooley, Math. Comput. **15**, 363 (1961).
[27]J. K. Cashion, J. Chem. Phys. **39**, 1872 (1963).
[28]S. O'Shea and W. Meath, Mol. Phys. **28**, 1431 (1974).
[29]For two physisorbed atoms at a separation r, we represent the damping function by $D(r) = a/(1 + b/r)$; $a = 100.07$, $b = 7.093$ A (Ref. 28).
[30]E. Merzbacher, *Quantum Mechanics* (Wiley, New York, 1970), p. 475.
[31]M. Abramowitz and I. Stegun, *Handbook of Mathematical Functions* (Dover, New York, 1968), p. 435.
[32]A. S. Davydov, *Quantum Mechanics* (Pergammon, Oxford, 1965), p. 609.
[33]I. S. Gradshteyn and I. M. Ryzhik, *Tables of Integrals, Series and Products*, 4th Ed. (Academic, New York, 1965).
[34]C. Douketis, G. Scoles, S. Marchetti, M. Zen, and A. J. Thakkar, J. Chem. Phys. **76**, 3057 (1982).
[35]G. Vidali, M. W. Cole, S. Rauber, and J. R. Klein, Chem. Phys. Lett. **95**, 213 (1983).
[36]D. M. Bishop and S. Shih, J. Chem. Phys. **64**, 162 (1976).
[37]K. K. Tang, J. M. Norbeck, and P. R. Certain, J. Chem. Phys. **64**, 3063 (1976).
[38]R. P. Bell, *The Tunnel Effect in Chemistry* (Chapman and Hall, London, 1980).
[39]In a recent paper on the rate of spin flip for physisorbed atomic hydrogen (Ref. 40), the present frozen-z approximation was used with the much less descriptive label of "$2\frac{1}{2}D$."
[40]J. P. H. W. v.d. Eijnde, C. J. Reuver, and B. J. Verhaar, Phys. Rev. B **28**, 6309 (1983).